

Eckels, S.J., T.M. Doerr, and M.B. Pate, *Heat transfer coefficients and pressure drops for R-134a and an ester lubricant mixture in a smooth tube and a micro-fin tube*. ASHRAE transactions, 1998. 104(1a): p. 366-375.

## **Heat Transfer Coefficients and Pressure Drops for R-134a and an Ester Lubricant Mixture in a Smooth Tube and a Micro-Fin Tube.**

S.J. Eckels                      T.M. Doer                      M.B. Pate  
Member ASHRAE              Student Member ASHRAE      Member ASHRAE

### **ABSTRACT**

This paper reports average heat transfer coefficients and pressure drops during evaporation and condensation of mixtures of R-134a and a 150 SUS penta erythritol ester branched-acid lubricant. The smooth tube and micro-fin tube tested in this study had outer diameters of 9.52 mm (3/8 in.). The micro-fin tube had 60 fins, a fin height of 0.2 mm (0.008 in), and a spiral angle of 18°. The objective of this study was: 1) to evaluate the effectiveness of the micro-fin tube with R-134a, and 2) to determine the effect of circulating lubricant.

The experimental results show that the micro-fin tube has distinct performance advantages over the smooth tube. For example, the average heat transfer coefficients during evaporation and condensation in the micro-fin tube were 50% to 200% higher than those for the smooth tube, while the average pressure drops were on average only 10% to 50% higher. The experimental results indicate that the presence of lubricant degrades the average heat transfer coefficients during both evaporation and condensation at high lubricant concentrations. Pressure drops during evaporation increased with the addition of lubricant in both tubes. For condensation, pressure drops were unaffected by additions of lubricant.

### **Key Words**

Evaporator, Condenser, Heat Transfer, Pressure Drop, Refrigerants

### **Primary Author**

Steven Eckels  
341 Durland Hall  
Manhattan, KS 66506-5106  
Phone: 913-532-5610  
Fax: 913-532-7057

## INTRODUCTION

Average heat transfer coefficients and pressure drops are reported for R-134a-lubricant mixtures in a smooth tube and a micro-fin tube. The test matrix included measurements for both evaporation and condensation over a mass flux range of  $85 \text{ kg/m}^2 \text{ s}$  ( $62,700 \text{ lb/ft}^2 \text{ hr}$ ) to  $375 \text{ kg/m}^2 \text{ s}$  ( $276,640 \text{ lb/ft}^2 \text{ hr}$ ). The 150 SUS penta erythritol ester branched-acid lubricant was tested over a concentration range of 0% to 5%. The average saturation temperatures during evaporation and condensation were  $1 \text{ }^\circ\text{C}$  ( $34 \text{ }^\circ\text{F}$ ) and  $40 \text{ }^\circ\text{C}$  ( $104 \text{ }^\circ\text{F}$ ), respectively. One goal of this study was to identify the effect ester lubricants have on the performance of R-134a in the test tubes. In addition, the overall performance of R-134a in the micro-fin tube was of interest.

This paper is the fourth in a series of papers reporting the results of ASHRAE research project 630-RP. The first paper (Eckels et al. 1993) reported solubility data for R-134a and the two ester type lubricants used in 630-RP. In that paper, measured solubility data was used to predict the temperature of refrigerant-lubricant mixtures in an evaporator or condenser tube. The second and third papers (Eckels et al. 1994a & 1994b) presented evaporation and condensation data for mixtures of R-134a and a penta erythritol ester mixed-acid lubricant in a smooth tube and a micro-fin tube. The penta erythritol ester mixed-acid lubricant was tested at viscosity levels of 169 SUS and 369 SUS. The present paper extends the results presented in the second and third papers to include a second ester type lubricant.

Since this paper is the fourth paper in a series, a number of the introductory topics have already been discussed in detail. For example, the previous studies conducted on R-134a were discussed in Eckels et al. (1994a & 1994b) and are not commented on here. This paper includes only a brief discussion of the experimental facility, the data reduction equations, and the experimental uncertainty since a detailed discussion appeared in Eckels et al. (1994a). The main focus of this paper is presentation and analysis of the experimental results, which is broken into three sections. First, the experimental data are presented and the effect of lubricant concentration discussed. Next, the performance of the micro-fin tube is analyzed by directly comparing the results with that of the smooth tube. Finally, empirical correlations are presented that can be used to predict the results presented in this paper.

## TEST FACILITIES

The test facility measures the average heat transfer coefficient and pressure drop of a fluid flowing through a test tube. The test facility has five main sections: the test section, the refrigerant loop, the water loop, the water-glycol loop, and the data acquisition system. Figure 1 shows a schematic diagram of the test facility and the layout of the main sections. The system allows the performance to be measured during either evaporation or condensation of a refrigerant or a refrigerant-lubricant mixture flowing in the 3.66 m (12 ft) long test tube. Lubricant is added to the system in a batch process and is circulated with the refrigerant during testing. Details of the lubricant injection and sampling process and a detailed description of all loops can be found in Eckels et al. (1994a).

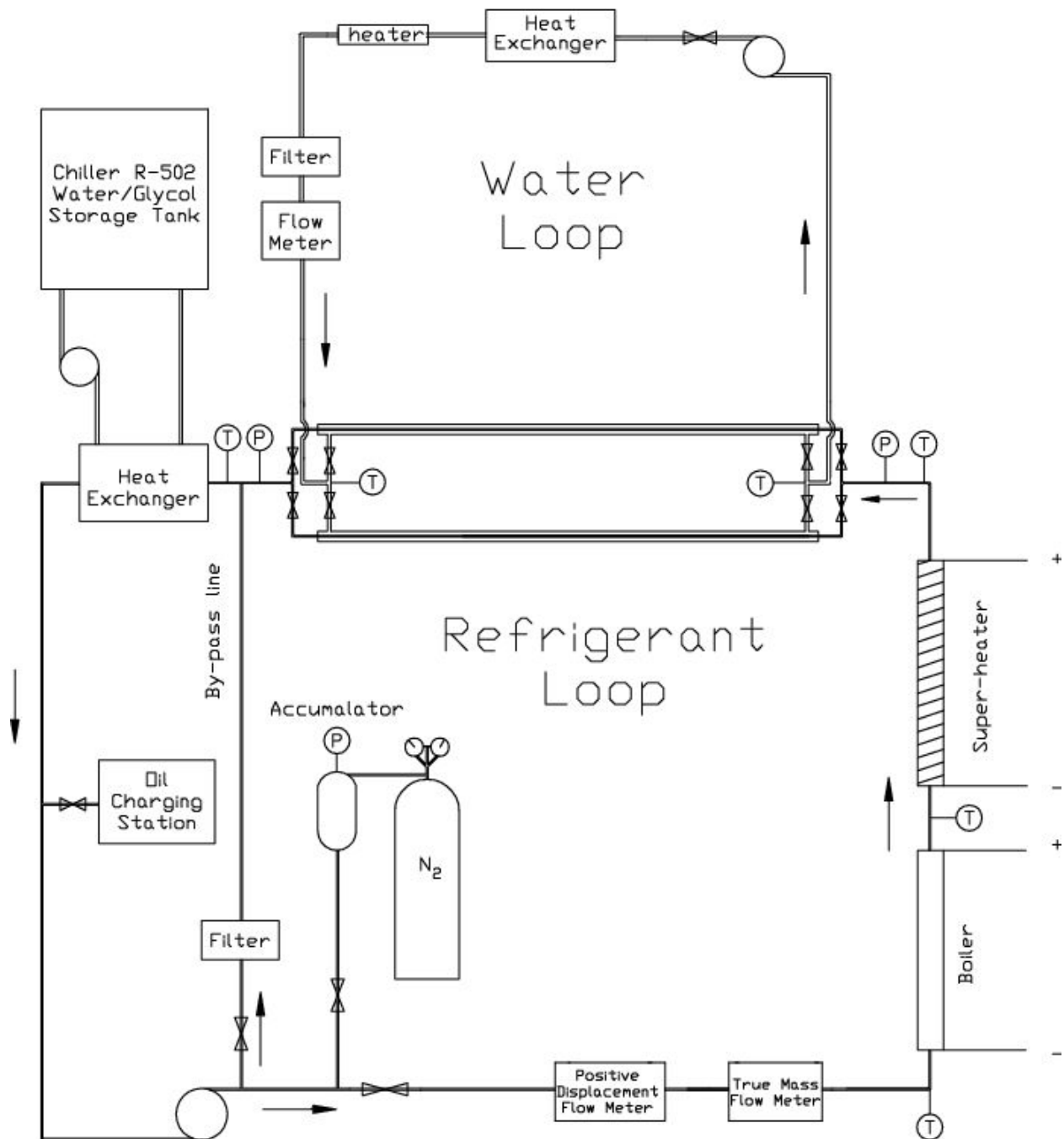


Figure 1: Schematic of test facility

The test section is composed of two tube-in-tube counter flow heat exchangers and instrumentation. Only one of the heat exchangers is active during testing. In the heat exchangers, water flows in the outer annulus and refrigerant in the inner test tube. Resistance Temperature Devices (RTDs) with an uncertainty of  $\pm 0.05$  C (0.09 F) measure the temperatures at the inlet and exit of the counter flow heat exchanger. The pressure of the refrigerant entering the heat exchanger is monitored with a pressure transducer with an uncertainty of  $\pm 2.1$  kPa (0.3 PSI), while the pressure drop across the test tube is measured with a differential pressure transducer.

The refrigerant loop circulates refrigerant through the test tube in the test section. The refrigerant exiting the test section is condensed and subcooled in the after-condenser. The water-glycol loop provides the cooling medium to the after-condenser. A positive displacement pump, which does not require lubricant for operation, circulates the subcooled refrigerant. A coriolis effect flow meter with an uncertainty of  $\pm 0.15\%$  measures the flow rate of refrigerant entering the test section. Before entering the test section, the refrigerant is heated to the desired temperature and quality in the boiler that is a 2.63 m (8.6 ft) long stainless steel tube heated by direct electrical current.

The water loop supplies water to the annulus side of the heat exchangers in the test section. A water pump circulates the water with flow control provided by a globe valve. During steady state, a heat exchanger and immersion heater in the water line balance the energy added or removed from the water in the test section. A coriolis effect flow meter measures the water flow rate with an uncertainty of  $\pm 0.15\%$ .

The data acquisition system monitors and records the output from all instrumentation in the test facility. The system uses a scanner, voltmeter, IEEE488 bus, and computer. During final data acquisition, output from each instrument in the system is measured five times and recorded. The average of the five readings for each channel is used in the data reduction.

## DATA REDUCTION

This section outlines the data analysis procedures used for pure refrigerants and refrigerant-lubricant mixtures. The data reduction equations calculate the average heat transfer coefficient on the inner surface of the test tube from the raw data supplied by the data acquisition system. In addition, data reduction equations calculate the quality at the inlet and exit of the test tube. The equations used for analysis of pure refrigerants are outlined first. The modified procedures used to analyze refrigerant-lubricant mixtures are discussed next. Finally, the uncertainties associated with the calculated heat transfer coefficients and measured pressure drops are presented.

### Pure Refrigerant

The average heat transfer coefficient on the inner surface of the test tube is calculated using a Log-Mean-Temperature-Difference (LMTD) type analysis on the counter flow heat exchanger. The definition of the overall heat transfer coefficient is

$$\frac{1}{UA} = \frac{1}{\varepsilon \cdot h_w \cdot A_w} + R_{Tube} + \frac{1}{\varepsilon \cdot h_r \cdot A_r} \quad (1),$$

where  $\varepsilon$  is the surface efficiency that accounts for the presence of fins,  $R_{tube}$  is the resistance of the copper tube, and  $A$  is the surface area of the tubes. For the smooth tube, the surface efficiency is 1 because no fins are present on either the inner or outer surface. Past convention for the micro-fin tube has been to model the inner finned surface as a smooth surface. Using a smooth surface model for the micro-fin tube, the surface efficiency becomes 1 and the surface area is based on the maximum inside diameter which is defined as the outer surface diameter minus twice the minimum wall thickness. The result of this simplification is that the heat transfer coefficient includes the surface area increase which is associated with the fins. The advantage of this method is that designers can apply the heat transfer coefficients without detailed knowledge of the surface structure. The surface area for the micro-fin tube used in this study was 1.5 times larger than that of a smooth tube with an equivalent inside diameter. Using

Equation 1 and realizing that the resistance of the copper tube is negligible gives the following formula for  $h_r$ :

$$h_r = \frac{1}{\left(\frac{1}{U_w} - \frac{1}{h_w}\right) \frac{A_r}{A_w}} \quad (2),$$

Equation 2 shows that the heat transfer coefficient on the inner surface can be calculated once the overall heat transfer coefficient and the annulus side heat transfer coefficient are known.

Heat transfer coefficients on the annulus side of the heat exchanger were measured with a Wilson plot technique (Eckels et al. 1994b). From the Wilson plot data, a correlation was developed that predicted the annulus side heat transfer coefficients given the water temperature and flow rate. The annulus correlation was specific to the flow rates and temperature used in this study. The overall heat transfer coefficient can be determined from the energy transferred in the test section and the log-mean-temperature-difference (LMTD).

$$U_w = \frac{Q}{LMTD \cdot A_w} \quad (3)$$

The energy transfer to the refrigerant ( $Q$ ) is calculated from the measured water flow rate and temperatures in the annulus. The LMTD is based on the water inlet and exit temperatures and the average saturation temperature of the refrigerant in the test tube. Since the refrigerant in the test section is a two-phase mixture, the average saturation temperature is based on the average pressure measured in the test tube.

### Refrigerant-Lubricant Mixtures

Data reduction for refrigerant-lubricant mixtures requires a few adjustments to the procedures outlined above. The properties of the refrigerant-lubricant mixture that are used during data analysis must be estimated from mixing equations such as those presented in Jensen and Jackman (1984). The presence of lubricant also changes the method used to calculate the LMTD. Specifically, calculating the average temperature in the test tube must account for the presence of lubricant. For the pure refrigerant, knowledge of the average pressure is sufficient for determining the average saturation temperature in the tube. The average temperature for a refrigerant-lubricant mixture must be determined with solubility data that relates pressure, temperature, and lubricant concentration. In this study, solubility data was used to calculate the average saturation temperature from the known average pressure and lubricant concentration (Eckels et al. 1993).

### Experimental Uncertainty

The uncertainty in the average heat transfer coefficients and pressure drops were calculated from the pure refrigerant data. A propagation of error analysis (Kline and McClintock 1953) was used to estimate the uncertainty in the average heat transfer coefficients. Table 1 shows typical ranges of uncertainty for the average heat transfer coefficients in the smooth tube and the micro-fin tube. The uncertainty in the pressure drop measurement was estimated statistically. During final data acquisition, the pressure drop across the tube was measured 35 times. The 35 pressure drop readings were used to calculate a 95% confidence interval on the mean pressure drop value. Table 2 lists typical values of the 95% confidence interval as a percent of the total reading. The large uncertainties associated with condensation pressure drops at low flow rates is due to the low absolute value of pressure drop. Specific uncertainties for

**Table 1: Uncertainty in Heat Transfer coefficient**

Mass Flux kg/m <sup>2</sup> s	Evaporation		Condensation	
	Smooth tube	Micro-fin tube	Smooth tube	Micro-fin tube
125	+9%	+14%	+9%	+13%
200	+8%	+12%	+6%	+10%
300	+7%	+10%	+5%	+8%
375	+7%	+9%	+5%	+8%

**Table 2: Uncertainty in pressure drop**

Mass Flux kg/m <sup>2</sup> s	Evaporation		Condensation	
	Smooth tube	Micro-fin tube	Smooth tube	Micro-fin tube
125	+11%	+11%	+25%	+30%
200	+6%	+5%	+16%	+18%
300	+3%	+4%	+12%	+9%
375	+2%	+3%	+9%	+7%

refrigerant-lubricant mixtures were not estimated. The uncertainty in the refrigerant-lubricant mixture results will be slightly higher than those for the pure refrigerant because of the additional uncertainty associated with estimating the saturation temperature with solubility data.

## Experimental Results

This section reports the average heat transfer coefficients and pressure drops during evaporation and condensation of R-134a-lubricant mixtures in the smooth tube and the micro-fin tube. The 150 SUS penta erythritol ester branched-acid lubricant was tested at concentrations of 0.0%, 1.2%, 2.4%, and 5.0%. Table 4 lists the range of flow rates, pressures, and qualities tested. The smooth tube and micro-fin tube were 3.66 m (12 ft) long with a 9.52 mm (3/8 in) outer diameter. The micro-fin tube has small symmetrical fins on the inner surface of the tube that are wider at the base with a narrow rounded tip. Micro-fin tubes have also been produced that have pointed tips, flat tips and even asymmetrical fin design. Table 3 gives additional information on the dimensions of tubes. The objective of this section is to present the experimental data and examine the effect lubricant concentration has on R-134a performance. A direct comparison of the smooth tube and micro-fin tube results is given in the next section.

A number of ratios are formed in the following sections to help identify significant trends in the data. Two main types of ratios are formed: the heat transfer enhancement factor (EF), which is a ratio of heat transfer coefficients, and the pressure drop penalty factor (PF), which is the ratio of pressure drops. An indexing system has been used to help identify which EF and PF ratios are being presented. A subscript "s" will designate smooth tube and "a" will represent micro-fin tube. A prime added to either subscript will denote that lubricant was present. For example,  $PF_{a'/s'}$  represents the pressure drops for refrigerant-lubricant mixtures in the micro-fin tube divided by the pressure drops for the refrigerant-lubricant mixture in the smooth tube at equivalent mass fluxes and lubricant concentrations.

### Evaporation

The average heat transfer coefficients during evaporation in the smooth tube and micro-fin tube are shown in Figure 2. The upper set of curves in the figure represents the micro-fin

**Table 3: Micro-fin tube and smooth tube dimensions**

	Micro-fin tube	Smooth tube
Outside Diameter, mm	9.52	9.52
Wall Thickness, mm	0.3	0.76
Maximum inside diameter, mm	8.92	8
Cross section area, mm <sup>2</sup>	58.1	50.3
Fin height, mm	0.2	--
Spiral Angle, °	17	--
Number of fins	60	--

**Table 4: Test conditions for smooth tube and micro-fin tube**

	Condensation	Evaporation
Temperature, °C	40	1
Pressure, MPa	1.01	0.33
Mass flux, kg/m <sup>2</sup> s	125 - 375	125-375
Quality in, %	80 - 88	5-15
Quality out, %	5 - 10	79-88
Lubricant Concentration, %	0 - 5	0-5

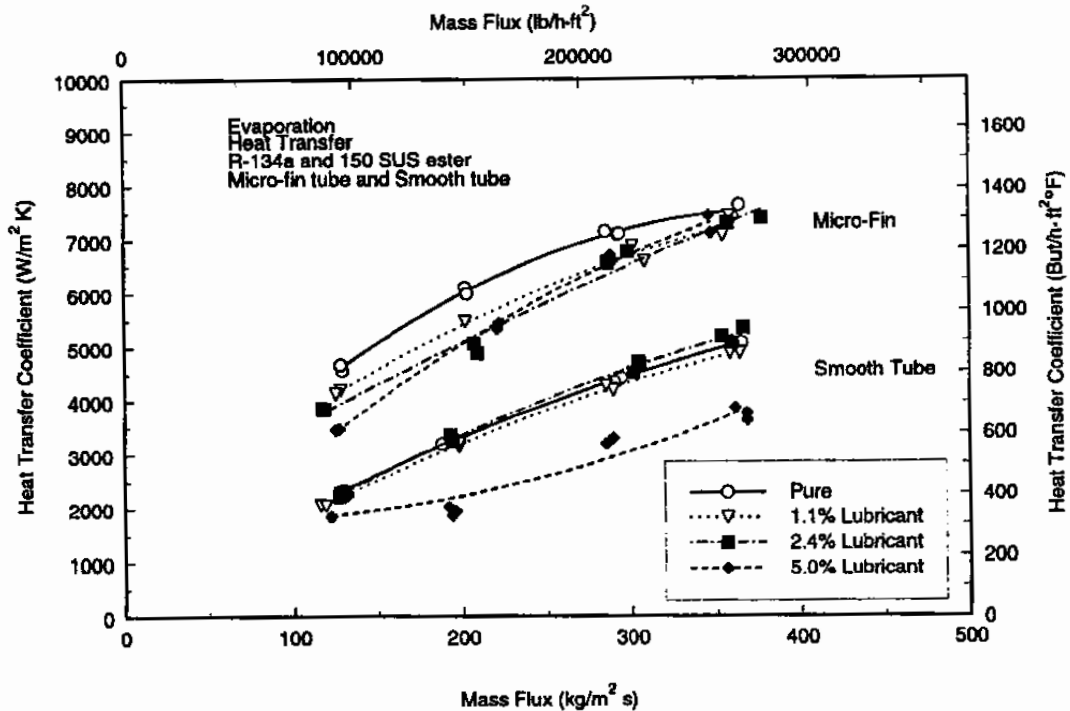


**Figure 2: Average heat transfer coefficients during evaporation in a 9.52 mm outer diameter smooth tube and micro-fin tube.**

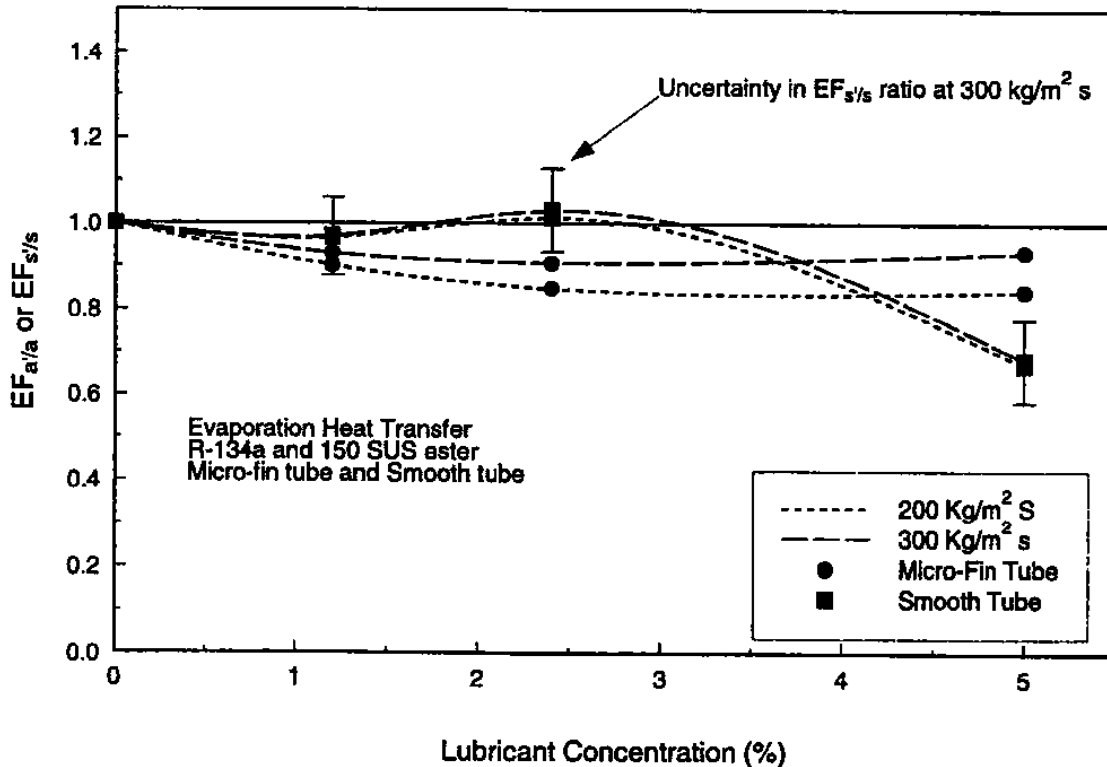


**Figure 3: Effect of lubricant concentration on heat transfer coefficients during evaporation in the smooth tube and micro-fin tube**

tube data and the lower set the smooth tube data. The lines shown on the plot are a second-order model with one independent variable (mass flux) fit with least squares to the data at each lubricant concentration. These results show that mass flux and lubricant concentration have a significant effect on the average heat transfer coefficient. The graph also shows that the heat transfer coefficients for the micro-fin tube are significantly larger than those for the smooth tube.

The effect of lubricant concentration can be isolated by forming the heat transfer enhancement factors  $EF_{s/s}$  and  $EF_{a/a}$ . The EF ratios are formed from the least square curve fits presented in Figure 2. The  $EF_{s/s}$  and  $EF_{a/a}$  ratios, shown in Figure 3, indicate that the addition of lubricant significantly decreases the average heat transfer coefficient at higher heat transfer coefficients. Figure 3 also shows the uncertainty associated with these ratios for one smooth tube line. At a 5% lubricant concentration, the  $EF_{a/a}$  ratio is 0.92 and 0.82 at the mass fluxes shown and the  $EF_{s/s}$  ratio is about 0.74.

Eckels et al. (1994a) presented similar results for mixtures of R-134a and a penta erythritol ester mixed-acid (ester-m) lubricant. The ester-m lubricant was tested in the same smooth tube and micro-fin tube at viscosity levels of 169 SUS and 369 SUS. For the 169 SUS lubricant, the  $EF_{a/a}$  and  $EF_{s/s}$  ratios ranged from 1.05 to 1.15 at the low lubricant concentrations and fell to values of 0.90 to 0.75 at a 5% lubricant concentration. The 150 SUS ester tested in this study did not show enhanced heat transfer at any lubricant concentration. The reasons for the difference in performance of these two lubricants have not yet been explained. Possible explanations are the differences in the mixtures' properties or differences in the foaming characteristics of the two lubricants.



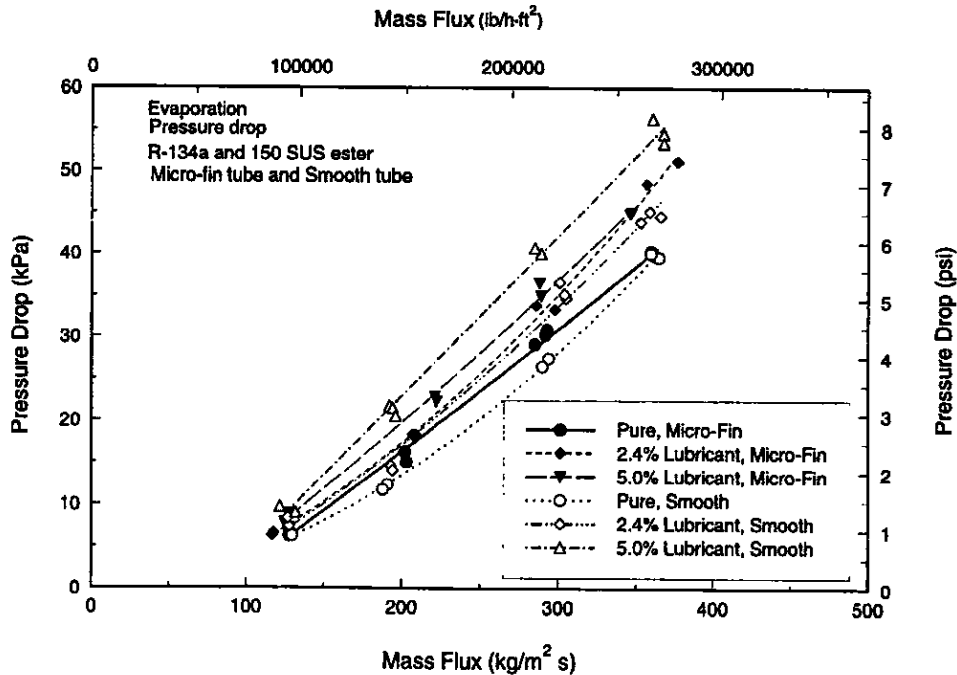


**Figure 4: Average pressure drop during evaporation in a 9.52 mm outer diameter smooth tube and micro-fin tube**

Figure 4 shows the pressure drops during evaporation of the R-134a/penta erythritol ester branched-acid (ester-b) lubricant mixture. The lines on the figure represent the pressure drop as a function of mass flux at each lubricant concentration. For both the smooth tube and the micro-fin tube, only three of the lubricant concentrations tested are shown (to help keep the data presentation clear). Pressure drops are shown to increase with mass flux and lubricant concentration. For pure R-134a, the pressure drops in the micro-fin tube are larger by about 4 kPa (0.6 PSI) at the middle mass fluxes and about the same at the higher and lower mass fluxes.

The evaporation pressure drop penalty factors  $PF_{s/s}$  and  $PF_{a/a}$  are shown in Figure 5. The  $PF_{s/s}$  and  $PF_{a/a}$  ratios increase with lubricant concentration for the three mass fluxes shown. The  $PF_{s/s}$  ratios show a more dramatic increase with lubricant concentration than the  $PF_{a/a}$  ratios do. For example, at a 5% lubricant concentration, the  $PF_{s/s}$  ratio ranges from 1.4 to 1.6, while the  $PF_{a/a}$  ratio is about 1.2. The  $PF_{s/s}$  ratio also decreases with mass flux at the higher lubricant concentrations. Results for mixtures of R-134a and an ester-m lubricant (Eckels et al. 1994a) were similar to those seen above. Specifically, the pressure drop penalty factor  $PF_{s/s}$  for the ester-m mixture was significantly higher than the  $PF_{a/a}$  ratio at the higher lubricant concentrations. In addition, the pressure drop penalty factors for the ester-m lubricant also showed a decreasing trend with mass flux.

### Condensation

The average heat transfer coefficients during condensation of the R-134a/ester-b lubricant mixtures are shown in Figure 6. The figure shows the micro-fin tube heat transfer coefficients to be significantly higher than those for the smooth tube. Figure 7 isolates the effect of lubricant concentration on the heat transfer coefficients during condensation. The  $EF_{s/s}$  and  $EF_{a/a}$  ratios decrease with lubricant concentration, with values of about 0.85 at a 5% lubricant

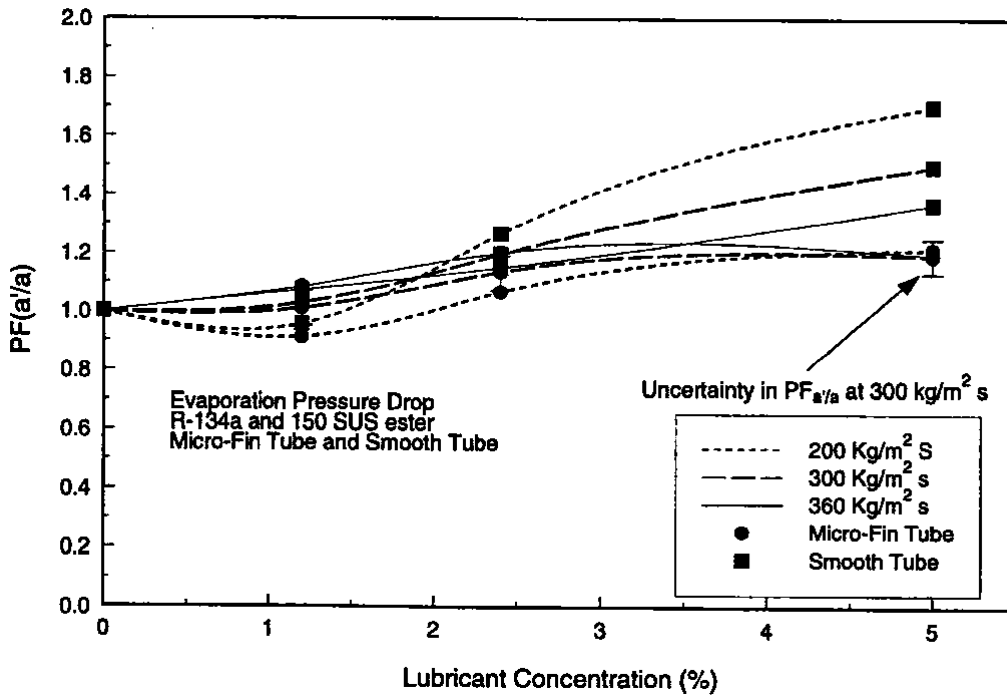


Figure 5: Effect of lubricant concentration on pressure drop during evaporation in the smooth tube and micro-fin tube.

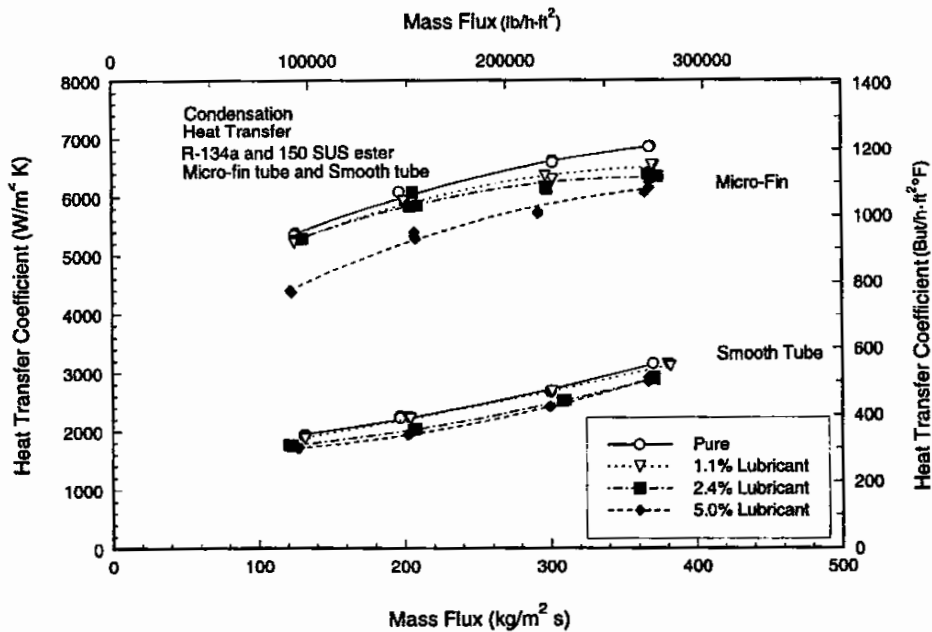
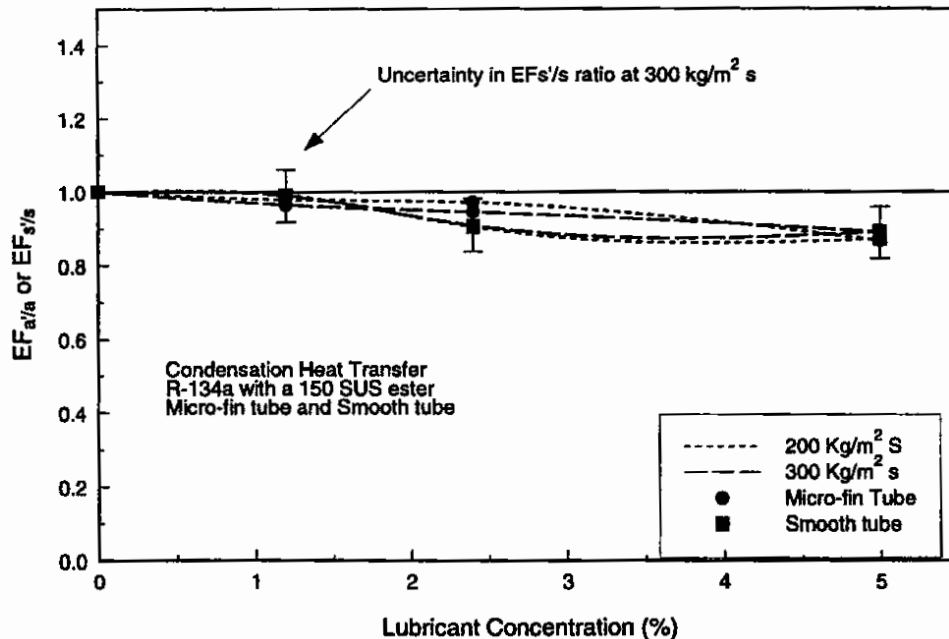


Figure 6: Average heat transfer coefficients during condensation in a 9.52 mm outer diameter smooth tube and micro-fin tube.



**Figure 7: Effect of lubricant concentration on heat transfer coefficients during condensation in the smooth tube and micro-fin tube.**

concentration. The uncertainty associated with these ratios are shown for the smooth tube ratio. Previously reported results for the ester-m lubricant (Eckels et al.1994b) also showed decreasing  $EF_{a/a}$  and  $EF_{s/s}$  ratios with lubricant concentration. For example, the  $EF_{s/s}$  ratio for the ester-m lubricant ranged from 0.8 to 0.85 at a 5% lubricant concentration.

Figure 8 shows the average pressure drops over the test tube during condensation. For pure R-134a, the micro-fin tube pressure drops are 0.5 kPa (0.07 PSI) larger than the smooth tube pressure drops at the low mass flux and 4 kPa (0.58 PSI) larger at the highest mass flux. Figure 9 presents the  $PF_{s/s}$  and  $PF_{a/a}$  ratios formed from the curves presented in Figure 8. The  $PF_{s/s}$  and  $PF_{a/a}$  have no distinguishable trends with lubricant concentration or mass flux. The  $PF_{a/a}$  and  $PF_{s/s}$  ratios vary from 1.2 to 0.95 over the range of lubricant concentrations tested. As noted by the error bars shown for one micro-fin tube line, the uncertainty in the ratio includes 1.0 for most data points.

Condensation pressure drops for refrigerant-lubricant mixtures have a large range of results cited in literature. Previous studies with mixtures of R-134a and polyalkylene glycol (Eckels and Pate 1991, Torikoshi and Kawabata 1992) showed that the addition of lubricant had little effect on condensation pressure drops. Yet Eckels et al. (1994b) showed that additions of a 169 SUS ester-m lubricant significantly increased pressure drop (<40% increase), while additions of a 369 SUS ester-m lubricant reduced condensation pressure drop. Similar type results can be found for other refrigerant-lubricant pairs. Two possible conclusions could be drawn from these results. The uncertainty in condensation pressure drop is masking the actual phenomenon occurring in the tube or interactions between the specific refrigerant-lubricant pair have a significant effect on pressure drops during condensation.

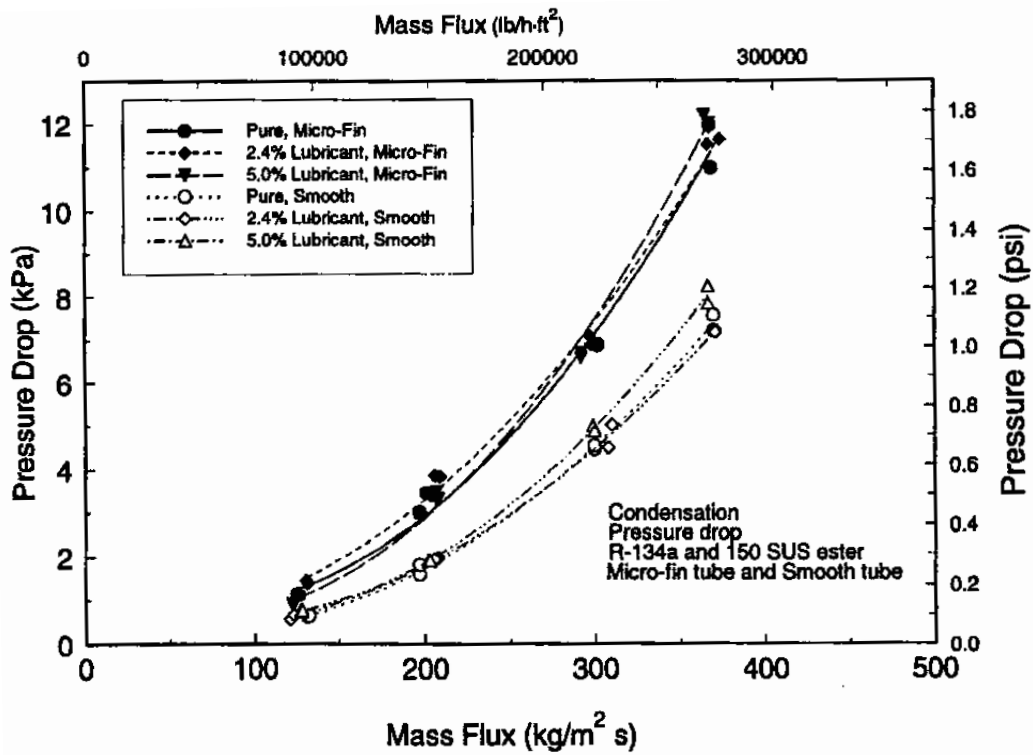


Figure 8: Average pressure drops during condensation in a 9.52 mm outer diameter smooth tube and micro-fin tube.

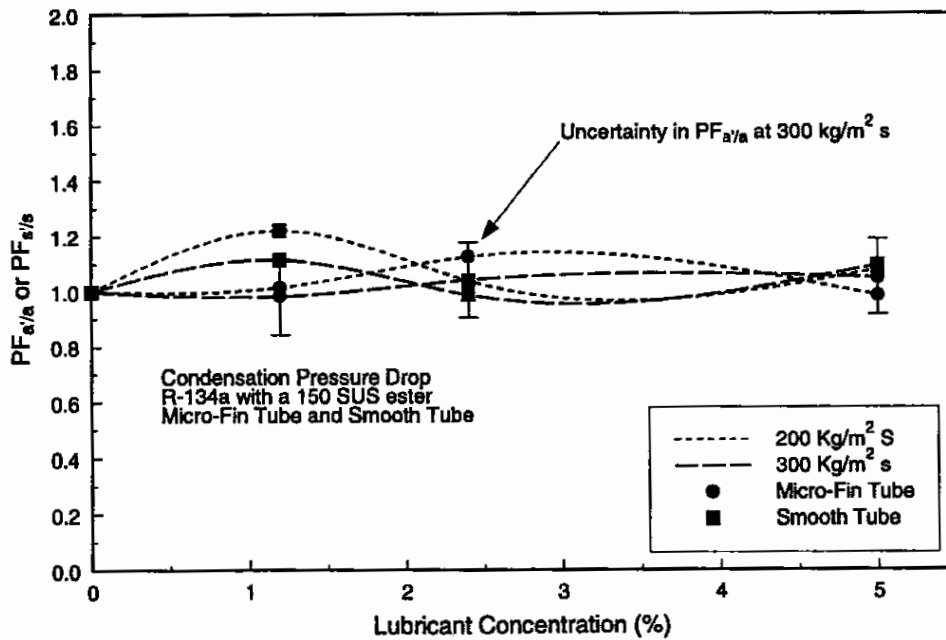


Figure 9: Effect of lubricant concentration on pressure drop during condensation in the smooth tube and micro-fin tube.

## Comparison of Smooth tube and Micro-fin tube

The objective in this section is to quantify the performance benefits of the micro-fin tube with R-134a. The relative performance of the micro-fin tube is determined by directly comparing the micro-fin tube and smooth tube results. For example, the pure R-134a performance is shown with the  $EF_{a/s}$  and  $PF_{a/s}$  ratios. These results can be extended to included lubricant mixtures by forming the  $EF_{a/s'}$  and  $PF_{a/s'}$  ratios. The heat transfer enhancement factors and pressure drop penalty factors presented in this section are formed using the least squares curve fits presented in Figures 2, 4, 6 and 8.

### Pure Refrigerant

The  $EF_{a/s}$  and  $PF_{a/s}$  ratios for evaporation of pure R-134a are shown in Figure 10. The  $EF_{a/s}$  values range from 2.0 at the lowest mass flux to 1.5 at the highest mass flux. The  $PF_{a/s}$  ratio shows a modest increase with ratio values ranging from 1.0 to 1.25. Previous results for evaporation in micro-fin tubes agree with the values given above. Torikoshi and Kawabata (1992) tested R-134a in a smooth tube and a micro-fin tube and found  $EF_{a/s}$  ratios that ranged from 2.5 at a mass flux of  $69 \text{ kg/m}^2 \text{ s}$  ( $50,890 \text{ lb/ft}^2 \text{ hr}$ ) to 2.0 at a mass flux of  $200 \text{ kg/m}^2 \text{ s}$  ( $147,500 \text{ lb/ft}^2 \text{ hr}$ ). Schlager et al (1989) reported the performance of R-22 in a smooth tube and a micro-fin tube and found the  $EF_{a/s}$  ratios that ranged from 2.3 to 1.8 over a mass flux range of  $125 \text{ kg/m}^2 \text{ s}$  ( $92,200 \text{ lb/ft}^2 \text{ hr}$ ) to  $400 \text{ kg/m}^2 \text{ s}$  ( $295,060 \text{ lb/ft}^2 \text{ hr}$ ).

Figure 11 shows the  $EF_{a/s}$  and  $PF_{a/s}$  ratios for condensation. The  $EF_{a/s}$  values range from 3.0 to 2.0, while the  $PF_{a/s}$  ratio varies from 2.0 to 1.5. The  $PF_{a/s}$  values at the higher mass fluxes where the uncertainty is lower is about 1.5. The  $PF_{a/s}$  ratio for condensation is significantly higher than that found during evaporation. It is interesting to note that the actual increase in pressure drop is less during condensation even though the ratio is higher. For example, at a mass flux of  $300 \text{ kg/m}^2 \text{ s}$  ( $221,280 \text{ lb/ft}^2 \text{ hr}$ ) the pressure drop during condensation in the micro-fin tube is 2.0 kPa (0.29 psi) higher than that of the smooth tube, while for evaporation the micro-fin tube pressure drop is 4.0 kPa (0.58 psi) higher than that for the smooth tube. Torikoshi and Kawabata (1992) also reported results for condensation of R-134a in a smooth tube and a micro-fin tube. The  $EF_{a/s}$  ratios for condensation appear to be about 2.68 at a mass flux of  $69 \text{ kg/m}^2 \text{ s}$  ( $50,890 \text{ lb/ft}^2 \text{ hr}$ ) and 3.0 at  $180 \text{ kg/m}^2 \text{ s}$  ( $132,700 \text{ lb/ft}^2 \text{ hr}$ ). They also reported condensation pressure drops in the smooth tube and micro-fin tube, and the  $PF_{a/s}$  ratios appear to be about 1.1 at  $69 \text{ kg/m}^2 \text{ s}$  ( $50,890 \text{ lb/ft}^2 \text{ hr}$ ) and 1.6 at a mass flux of  $180 \text{ kg/m}^2 \text{ s}$  ( $132,700 \text{ lb/ft}^2 \text{ hr}$ ).

### Refrigerant-Lubricant Mixtures

The effect of lubricant concentration on the micro-fin tube and smooth tube comparison is quantified by forming  $EF_{a/s'}$  and  $PF_{a/s'}$  ratios. Figure 12 shows the  $EF_{a/s'}$  and  $PF_{a/s'}$  ratios plotted versus lubricant concentration for two of the mass fluxes tested during evaporation. The  $EF_{a/s'}$  ratio is about constant for lubricant concentrations of 1.2% and 2.4%, then has an increase at the highest lubricant concentration. The increase in the  $EF_{a/s'}$  ratio is a direct result of the large drop in heat transfer coefficients for the smooth tube at the highest lubricant concentration (see Figure 3). The  $PF_{a/s'}$  ratio for evaporation is approximately constant.

Figure 13 shows results for condensation. The  $EF_{a/s'}$  ratio for condensation is approximately constant over the whole range of lubricant concentrations. The  $PF_{a/s'}$  ratio for condensation oscillates about the mean value but shows no definite trend with lubricant concentration. The general conclusion is that the performance benefits of the micro-fin tube are maintained with the addition of lubricant.

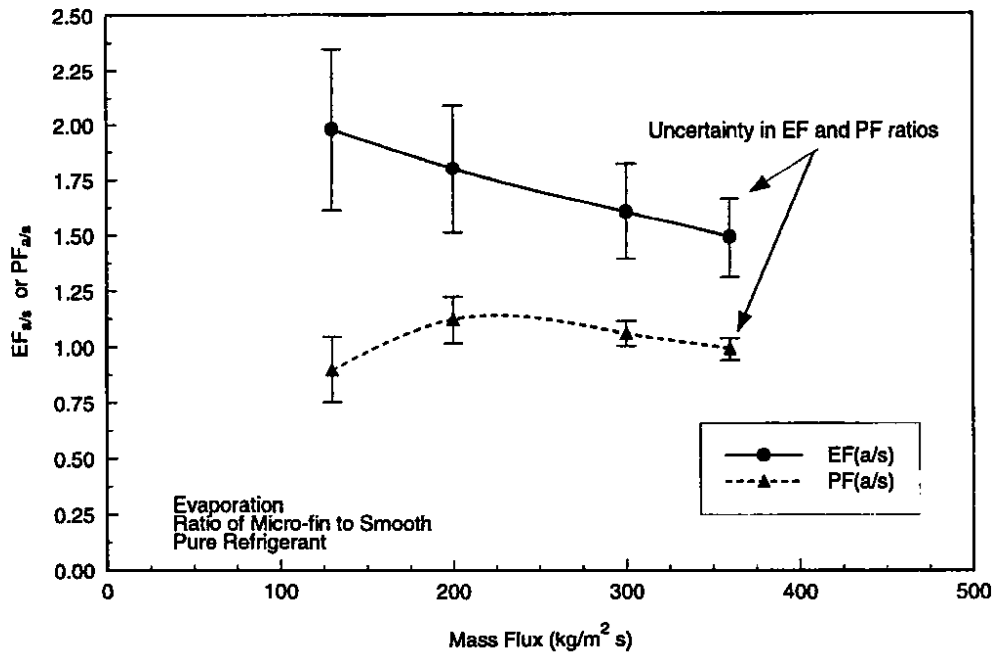


Figure 10: Comparison of micro-fin tube and smooth tube performance during evaporation for pure refrigerant.

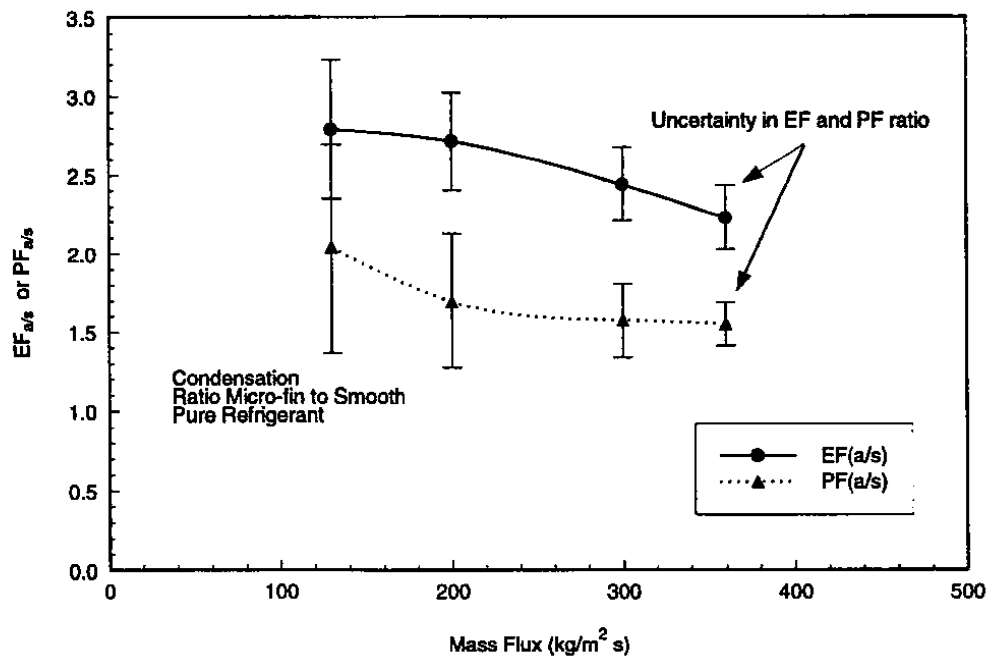


Figure 11: Comparison of micro-fin and smooth tube performance during condensaiton for pure refrigerant

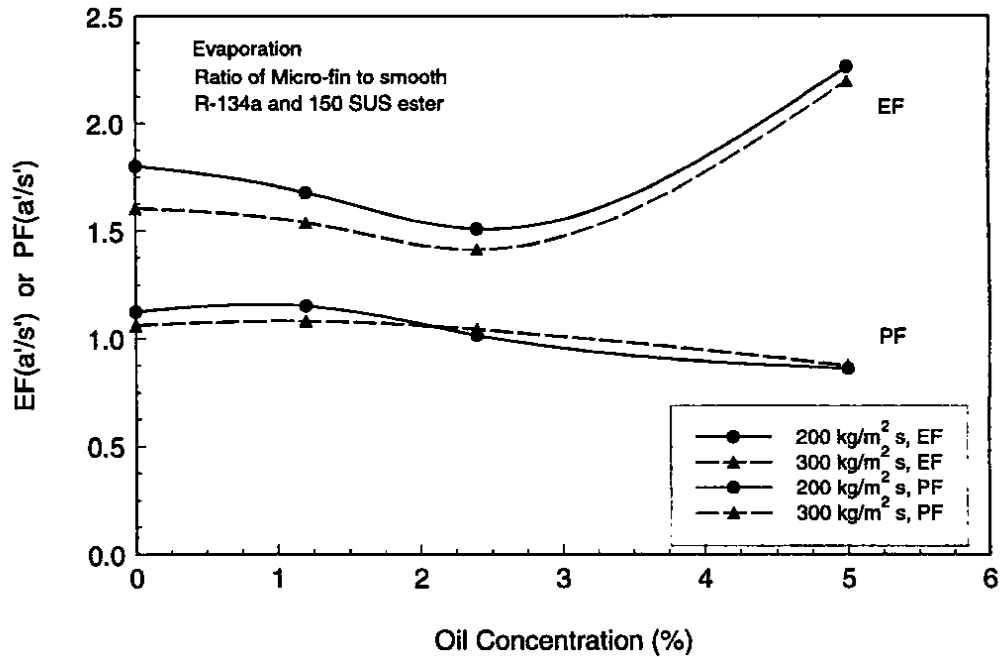


Figure 12: Effect of lubricant concentration of micro-fin tube and smooth tube performance during evaporation.

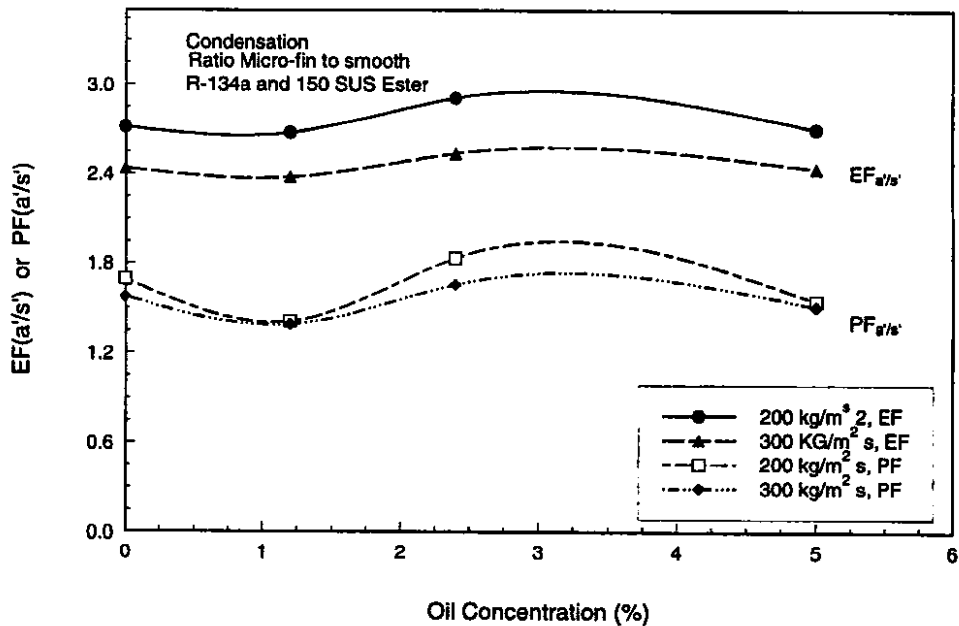


Figure 13: Effect of lubricant concentration on micro-fin tube and smooth tube performance during condensation.

Figure 13

## Design Equations

The design equations presented in this section are empirical curve fits of EF and PF ratios. The goal was to produce a correlation that would predict results for refrigerant-lubricant mixtures with smooth tube pure refrigerant data. The four ratios ( $EF_{s'/s}$ ,  $PF_{s'/s}$ ,  $EF_{a'/s}$ , and  $PF_{a'/s}$ ) were calculated by dividing refrigerant-lubricant mixture results by the pure refrigerant smooth tube results. The least square curve fits presented in Figures 2, 4, 6 and 8 were used to calculate the ratios. The experimentally determined ratios were then curve-fit to empirical correlations that used the refrigerant mass flux and lubricant mass fraction as variables. Application of the correlations developed in this section is limited to the range of conditions used in this study.

The design equations are used in the following manner. Pure refrigerant results in the smooth tube are multiplied by the appropriate heat transfer enhancement factor or pressure drop penalty factor to obtain the desired heat transfer coefficient or pressure drop. For example, if the heat transfer coefficients during evaporation of a refrigerant-lubricant mixture in the micro-fin tube were desired, then the following formula would be used:

$$h_{TP} = EF_{a'/s} \cdot h_{smooth} \quad (4)$$

where  $h_{TP}$  is the desired heat transfer coefficient and  $h_{smooth}$  a smooth tube heat transfer coefficient for the pure refrigerant during evaporation. The diameter of the smooth tube used to calculate the heat transfer coefficients should be the same as the maximum inside diameter of the micro-fin tube. Since the data used to generate the EF and PF ratios were averages over the test tube, the correlations should also only be applied to average heat transfer coefficients.

Two different correlations were developed for each EF and PF ratio. The correlations are second degree polynomials in normalized refrigerant mass flux and lubricant mass fraction with interactions terms:

$$EF \text{ or } PF = a_0 + a_1(\omega_l) + a_2(\omega_l G') + a_3(\omega_l^2 G') + a_4(\omega_l G'^2) + a_5(\omega_l^2 G'^2) + a_6(\omega_l^2) \quad (5)$$

$$\ln(EF) \text{ or } \ln(PF) = b_0 + b_1(\omega_l) + b_2(\omega_l G') + b_3(\omega_l^2 G') + b_4(\omega_l G'^2) + b_5(\omega_l^2 G'^2) + b_6(\omega_l^2) \quad (6)$$

where  $G'$  is calculated from

$$G' = \frac{G}{250} \quad (7)$$

A statistical analysis computer package was used to do the regression analysis on the data. The statistical methods used to develop the correlations are described in Eckels et al. (1994a). The final constants used in the regression analysis were a subset of Equations 5 and 6. A pre-analysis of the data by the statistics program selected the constants in Equations 5 and 6 that should be used in the final regression analysis. The goal was to selected the minimum set of constants that gave a high  $R^2$  value. The smooth tube EF and PF ratios also had a few special considerations. Specifically, the smooth tube EF and PF ratios must reduce to 1.0 when no lubricant was present. This limiting case was guaranteed by eliminating all mass flux terms from the correlation except those appearing in the interaction terms. For the micro-fin tube, the EF or



PF ratios do vary with mass flux at a 0% lubricant concentration (see Figures 10 & 11), so the mass flux terms were included.

Table 5 shows the EF and PF constants derived for Equation 5. The constants for Equations 6 are shown in Table 6. For each EF and PF ratio, a number of constants are listed as zero in Tables 5 and 6, which indicates they were not used in the regression analysis.

**Table 5: Constants for Equation 5**

	Evaporation Heat Transfer		Evaporation Pressure Drop		Condensation Heat Transfer		Condensation Pressure Drop	
	EF <sub>s/s</sub>	EF <sub>a/s</sub>	PF <sub>s/s</sub>	PF <sub>a/s</sub>	EF <sub>s/s</sub>	EF <sub>s/s</sub>	PF <sub>s/s</sub>	PF <sub>a/a</sub>
a0	1	2.45	1	0.41	1	2.8	1	1.84
a1	3.96	29.95	11.33	7.4	4.23	3.66	0	37.27
a2	0	1.01	0	1.21	0	0.19	0	0.22
a3	0	14.87	9.99	0	0	0	0	28.57
a4	411	0	768	0	86.65	337.9	0	647.4
a5	0	0	0	0	0	6.19	0	0
a6	202.1	50.28	504.8	36.01	51.08	0	0	0
a7	0	194.7	0	0	67.05	399.6	0	801.1
a8	0	0.24	0	0.55	0	0.41	0	0
R <sup>2</sup>	0.93	0.99	0.94	0.85	0.91	0.99	--	0.86

**Table 6: Constants for Equation 6**

	Evaporation Heat Transfer		Evaporation Pressure Drop		Condensation Heat Transfer		Condensation Pressure Drop	
	EF <sub>s/s</sub>	EF <sub>a/s</sub>	PF <sub>s/s</sub>	PF <sub>a/s</sub>	EF <sub>s/s</sub>	EF <sub>s/s</sub>	PF <sub>s/s</sub>	PF <sub>a/a</sub>
b0	0.00	0.98	0.00	0.56	0.00	1.00	0.00	0.62
b1	4.95	12.78	7.26	6.72	4.39	1.77	0.00	21.22
b2	0.00	0.63	0.00	1.12	0.00	0.14	0.00	0.14
b3	0.00	6.20	0.00	0.00	0.97	0.00	0.00	16.36
b4	498.50	143.60	701.40	0.00	0.00	140.10	0.00	3.77
b5	0.00	0.00	5.61	0.00	0.00	2.84	0.00	0.00
b6	245.20	78.37	478.50	34.27	57.15	0.00	0.00	0.00
b7	0.00	26.56	0.00	0.00	71.07	165.00	0.00	461.70
b8	0.00	0.17	0.00	0.51	0.00	0.20	0.00	0.00
R <sup>2</sup>	0.94	0.99	0.94	0.84	0.91	0.99	--	0.91

## CONCLUSIONS

Average heat transfer coefficients and pressure drops during evaporation and condensation were reported for mixtures of R-134a and a penta erythritol ester branched-acid lubricant. The mixture was tested over a lubricant concentration range of 0% to 5%. Mass fluxes in the smooth tube and micro-fin tube were varied from 125 kg/m<sup>2</sup> s (92,200 lb/ft<sup>2</sup> hr) to

375 kg/m<sup>2</sup> s (276,600 lb/ft<sup>2</sup> hr). The goal of this work was to determine the effectiveness of the micro-fin tube with R-134a and to evaluate the effect which circulating lubricants have on performance. Design equations were also developed to help predict the results obtained in this study.

The additions of the penta erythritol ester-b branched-acid lubricant decreased heat transfer coefficients during evaporation in the micro-fin tube. In the smooth tube, the heat transfer coefficients during evaporation were not affected by the addition of lubricant at low lubricant concentrations but were degraded at high lubricant concentrations. During condensation, the average heat transfer coefficients were degraded in both the smooth tube and micro-fin tube, with a 15% reduction in heat transfer coefficients at a 5% lubricant concentration. Evaporation pressure drops were increased in both the smooth tube and the micro-fin tube with the addition of the ester-b lubricant. Pressure drops during condensation did not show a significant effect from the addition of lubricant.

The micro-fin tube did show significant performance benefits over the smooth tube. During evaporation, the heat transfer coefficients were increased by 100% to 50%, while the pressure drops were only increased by 0% to 20%, over the mass flux range. During condensation, heat transfer coefficients in the micro-fin tube during condensation were increased by 200% to 100% over the smooth tube results but also had 100% to 50% higher pressure drop. The addition of lubricant did not have a significant effect on this performance comparison.

## ACKNOWLEDGMENTS

Support for this project was provided by ASHRAE Research Project RP-630. The guidance provided by the Sponsoring Technical Committee, TC 1.3, Heat Transfer and Fluid Flow, and the Project Monitoring Committee (Dr. Naim Azer, Mr. Keith Starner, and Dr. Lynn Schlager) is greatly appreciated. The contribution of test tubes by Wolverine Tube Company is also appreciated.

## NOMENCLATURE

A= Surface area  
a<sub>0</sub>-a<sub>6</sub> = Equation 5 constants  
b<sub>0</sub>-b<sub>6</sub>= Equation 6 constants  
G= Mass flux  
G'= Normalized mass flux  
h= Heat transfer coefficient  
T= Temperature  
U= Overall heat transfer coefficient

Greek Symbols  
ε= Surface efficiency  
ω= Lubricant mass fraction

## Subscripts

a= Pure refrigerant, micro-fin tube  
a'= Refrigerant-lubricant, micro-fin tube  
i= Inner surface

o= Outer surface  
s= Pure refrigerant, smooth tube  
s'= Refrigerant-lubricant, smooth tube  
r= Refrigerant  
w= Water

## REFERENCES

- Eckels, S.J., T.M. Doer, and M.B. Pate. 1994a. In-tube heat transfer and pressure drop of R-134a and ester lubricant mixtures in a smooth tube and a micro-fin tube: Part 1 evaporation. *ASHRAE TRANSACTIONS* 100 (2): 265-282.
- Eckels, S.J., T. M. Doer, and M. B. Pate. 1994b In-tube heat transfer and pressure drop of R-134a and ester lubricant mixtures in a smooth tube and a micro-fin tube: Part 1 condensation. *ASHRAE TRANSACTIONS* 100 (2): 283- 294.
- Eckels, S.J., S. C. Zoz, and M. B. Pate. 1993. Using solubility data for HFC-134a and ester lubricant mixtures to model an in-tube evaporator or condenser. *ASHRAE TRANSACTIONS* 99 (2) (1993): 283-391.
- Eckels S.J., and M. B. Pate. 1991. In-tube evaporation and condensation of refrigerant-lubricant mixtures of HFC-134a and CFC-12. *ASHRAE Transactions* 97 (2): 62-71.
- Jensen, M. K., and D. L. Jackman. 1984. Predictions of nucleate pool boiling heat transfer coefficients of refrigerant-oil mixtures. *Journal of Heat Transfer* 106: 184-190.
- Kline, S. J., and F. A. McClintock. 1953. Describing uncertainties in single sample experiments. *Mechanical Engineering* 75: 3-8.
- Torikoshi, K. and K. Kawabata. 1992. Heat transfer and pressure drops characteristics of HFC-134a in a horizontal heat transfer tube. In: *Proceedings: 1992 International Refrigeration Conference - Energy Efficiency and New Refrigerants* 1: 167-176.
- Schlager, L.M., M.B. Pate, and A. E. Bergles. 1989. Heat Transfer and Pressure Drop Performance of Smooth and Internally Finned Tubes with Oil and Refrigerant 22 Mixtures. *ASHRAE Transactions* 95(2): 375-423 .